Available online at www.sciencedirect.com

SciVerse ScienceDirect

Ceramics International 39 (2013) 6713–6720

CERAMICS INTERNATIONAL

www.elsevier.com/locate/ceramint

Effect of strontium and phosphorus source on the structure, morphology and luminescence of $Sr_5(PO_4)_2SiO_4:Eu^{2+}$ phosphor prepared by solid-state reaction

Keke Huang, Taoli Deng, Shirun Yan*, Jianguo Hu

Department of Chemistry and Fudan-Keheng Research Center for Luminescent Materials, Fudan University, Shanghai 200433, PR China

Received 17 January 2013; received in revised form 31 January 2013; accepted 31 January 2013
Available online 7 February 2013

Abstract

$Sr_5(PO_4)_2SiO_4:Eu^{2+}$ phosphosilicate phosphor was prepared by high temperature solid-state reaction. Effects of strontium sources (strontium oxide, strontium nitrate and strontium carbonate) and of phosphorus sources (diammonium phosphate, strontium monophosphate) on the reactivity of their mixture during heating and on phase composition, morphology and photoluminescence excitation and emission properties of the phosphors were investigated by TG–DTG–DSC, XRD, SEM and photoluminescence spectroscopy. The sequence of the solid-state reactions when using the different starting reagents was discussed based on the TG–DTG–DSC results. It was found that it is hard to prepare pure $Sr_5(PO_4)_2SiO_4:Eu^{2+}$ phosphor with either of strontium sources studied when stoichiometric $(NH_4)_2HPO_4$ was used as a phosphorus source. Minor Sr_2SiO_4 impurity phase was present in the phosphors. The content of impurity phase, the morphology and resultant photoluminescence properties of the phosphors were markedly influenced by the strontium source employed. When $SrCO_3$ was used as the strontium source, the phase purity of the phosphor was improved with the addition of excess $(NH_4)_2HPO_4$. When $(NH_4)_2HPO_4$with 5% excess or $SrHPO_4$ in stoichiometric ratio was used as the phosphorus source a pure phase phosphor was obtained. In addition, the morphology and photoluminescence of the phosphor were also influenced by phosphorus source. The possible reasons causing different properties of the phosphors prepared using different raw materials were discussed based on reaction schemes.

Keywords: $Sr_5(PO_4)_2SiO_4:Eu^{2+}$ phosphor; Strontium and phosphorus source; Structure; Morphology; Photoluminescence

1. Introduction

In recent years, growing interest has been focused on phosphor converted white light-emitting diodes (pc-WLEDs) for lighting because of their advantages of energy-saving, reliability, maintenance and safety [1,2]. Of the two alternative approaches to assemble pc-WLEDs, the nUV chip coated with blend of tri-chromatic phosphors or single-phased full-color phosphor approach is considered more competitive in terms of color uniformity, color rendition and long term color stability. Since nUV (350–420 nm) radiation of the chip is not perceived well by human eye, the emission color of WLED is controlled only by the phosphors [3]. On the other hand, the efficacy of WLEDs based on nUV chip is lower than that based on the blue platform mainly owing to Stokes shift losses. It is of great significance to find novel efficient phosphors that are able to absorb nUV light and convert it into a visible light with suitable spectrum. For this purpose, various silicate and nitride [2,4–9], phosphate [10–16], and phosphosilicate [17–22] singly doped with Eu^{2+} or Ce^{3+} or doubly-doped with Eu^{2+} and Mn^{2+} have been studied extensively as nUV pumping phosphors. The structure, photoluminescence mechanism and properties, as well as temperature-dependent photoluminescence in these phosphors have been investigated thoroughly. To be a phosphor candidate for actual application in pc-WLEDs, in addition to having a suitable shape and position of the emission and excitation spectra and good thermal quenching behavior, high external quantum efficiency is of the utmost importance to efficacy of the WLEDs. The quantum efficiency

*Corresponding author. Tel./fax: +86 21 65643987.
E-mail addresses: sryan@fudan.edu.cn, yanshirun@126.com (S. Yan).

0272-8842/$ - see front matter © 2013 Elsevier Ltd and Techna Group S.r.l. All rights reserved.
http://dx.doi.org/10.1016/j.ceramint.2013.01.113

of a phosphor is dependent on not only the internal quantum efficiency but also the absorbed fraction of the excitation light [23]. The absorption of excitation light is mainly influenced by dopant concentration and phase purity of a phosphor, the physical parameters of a phosphor such as, morphology, particle size and particle size distribution play an important role as well. In general, conversion phosphors for WLED are fabricated by solid-state reaction methods, the types of ingredient species employed may influence the reaction and nucleation mechanism and hence physicochemical and photoluminescence properties of the phosphors [24]. Therefore, investigation and understanding of the influence of raw materials and manufacturing process on the structure and property of the phosphor is of great industrial importance.

$Sr_5(PO_4)_2SiO_4:Eu^{2+}$ is a green emitting phosphor with an apatite structure firstly reported by Blasse and Bril in 1969 [25]. It was recently reported that $Sr_5(PO_4)_2SiO_4:Eu^{2+}$ was a potential candidate phosphor for nUV–WLED efficiently excitable in the wavelength range of 250–440 nm [19–21]. Synthesis of $Sr_5(PO_4)_2SiO_4:Eu^{2+}$ involved in the introduction and reactions of strontium, phosphorus and silica species. In this work, the $Sr_5(PO_4)_2SiO_4:Eu^{2+}$ phosphor was prepared by solid-state reaction with different strontium [SrO, $SrCO_3$, $Sr(NO_3)_2$] and phosphorus [$(NH_4)_2HPO_4$ and $SrHPO_4$] sources. The effects of strontium and phosphorus source on the reactivity of their mixture during heating and resultantly on the structure, morphology and photoluminescence excitation and emission properties of the phosphor were investigated.

2. Experimental

The phosphor with a composition of $Sr_{4.94}(PO_4)_2SiO_4:Eu^{2+}_{0.06}$ was prepared by a solid-state reaction technique. The starting materials were $SrCO_3$ (99%), SrO (99%), $Sr(NO_3)_2$ (>98%), SiO_2 (99.9%), $(NH_4)_2HPO_4$ (>99%), $SrHPO_4$ (99%), Eu_2O_3 (99.99%) and NH_4HF_2 (>98%). Assay was run on SiO_2 to compensate for sorbed water. The required amount of raw materials and NH_4HF_2 flux in amount of 1 wt% of the phosphor batch were thoroughly mixed and ground in an agate mortar.

Thermal analysis of the intimate mixture of raw materials was performed in a TA SDT Q600 instrument in air at a heating rate of 10 °C/min from room temperature up to 1300 °C. The instrument used in the investigations allows to carry out thermo gravimetric (TG), differential thermo gravimetric (DTG) and differential scanning calorimetric (DSC) analyses simultaneously.

Based on the thermal analysis results, the firing procedure of the intimate mixture of the starting reagents was determined. It was fired in air at 350 and 850 °C for 5 h with milling between two firing steps. The resultant powder was finally fired at 1350 °C in a H_2/N_2 atmosphere (5vol% of H_2) for 15 h. The sample was then allowed to cool in the reducing atmosphere to room temperature.

The X-ray diffraction (XRD) patterns of the phosphors were recorded on a Bruker D8 advance diffractometer with Cu Kα radiation ($\lambda = 0.15418$ nm) operated at 40 mA and 40 kV. The scanning electron microscopy (SEM) images of the phosphors were recorded on a Philips XL-30 scanning electron microscope. The photoluminescence excitation (PLE) and emission (PL) spectra of the phosphors were recorded using a Hitachi F-4500 fluorescence spectrophotometer at room temperature.

3. Results and discussion

3.1. Effect of strontium sources

Fig. 1 shows TG–DTG–DSC profiles of the stoichiometric mixture $Sr_{4.94}(PO_4)_2SiO_4:Eu_{0.06}$ of raw materials with different strontium sources using diammonium phosphate as the phosphorus source. When SrO was used as the strontium source, small endothermic and exothermic peaks accompanied by obvious weight loss steps appeared at temperature ranges of 140–210 (weight loss about 15%), 400–500 (weight loss about 5%) and 800–890 °C (weight loss about 3%), respectively. Since the ingredients SrO, SiO_2 and Eu_2O_3 were stable during heating, the species decomposable in the mixture were $(NH_4)_2HPO_4$ and NH_4HF_2 flux. Given that the amount of flux was only 1% of the total mixture, the weight losses in TGA curve should be ascribed to the degradation and decomposition of $(NH_4)_2HPO_4$ and subsequent reactions between degraded species and other ingredients in the mixture. It was seen from the DSC curve that highly exothermic reactions of ingredients took place at temperature range of 800–1300 °C. Based on the

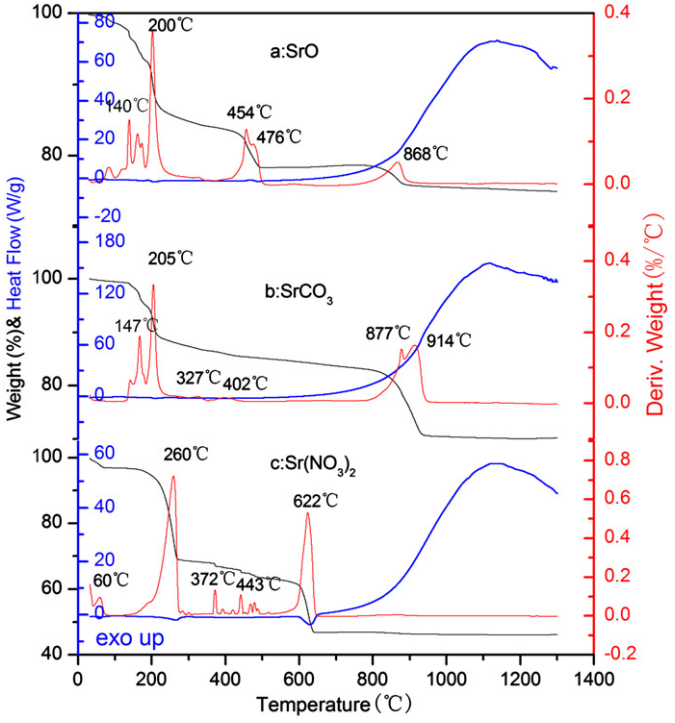

Fig. 1. TG–DTG–DSC profiles of stoichiometric mixture of raw materials with different strontium sources.

TG–DTG–DSC results and the chemistry of alkaline earth phosphates [26], the sequence of solid-state reactions taking place at different temperature ranges during heating of the stoichiometric mixture using SrO as the strontium source was proposed in the following equations:

$$(NH_4)_2HPO_4 \xrightarrow{\sim 140\ ^\circ C} H_3PO_4 + 2NH_3 \quad (1)$$

$$3H_3PO_4 + 2SrO \xrightarrow{140-200\ ^\circ C} SrHPO_4 + Sr(H_2PO_4)_2 + 2H_2O \quad (2)$$

$$2SrHPO_4 \xrightarrow{450-480^\circ C} Sr_2P_2O_7 + H_2O \quad (3)$$

$$Sr(H_2PO_4)_2 \xrightarrow{450-480^\circ C} SrH_2P_2O_7 + H_2O \quad (4)$$

$$2SrO + SiO_2 \xrightarrow{\sim 800-1300^\circ C} Sr_2SiO_4 \quad (5)$$

$$Sr_2SiO_4 + 5/3SrO + 1/3Sr_2P_2O_7 + 2/3SrH_2P_2O_7 \xrightarrow{\sim 800-1300^\circ C} Sr_5(PO_4)_2SiO_4 + 2/3H_2O \quad (6)$$

When $SrCO_3$ was used as the strontium source, two sharp weight loss steps at temperature ranges of 140–250 (weight loss about 12%) and 800–950 °C (weight loss about 13%) were observed. Other two weight loss steps with smaller weight loss percentage at temperature range of 300–450 °C were also observed in the DTG profile. No obvious weight loss was observed above 950 °C. Since both $SrCO_3$ and $(NH_4)_2HPO_4$ were reactive and degradable species, the weight loss steps in TGA curve could be ascribed to the degradation and reactions concerning $(NH_4)_2HPO_4$ and $SrCO_3$ species. Based on TG–DTG–DSC results and the chemistry of alkaline earth phosphates [26], the scheme of solid-state reactions at different temperature ranges during heating of the stoichiometric mixture using $SrCO_3$ as the strontium source was proposed as follows:

The initial weight loss step at 140 °C should be ascribed to the decomposition of $(NH_4)_2HPO_4$ as given in Eq. (1), followed by the reaction of H_3PO_4 with $SrCO_3$ at 200–250 °C leading to the formation of $SrHPO_4$ and $Sr(H_2PO_4)_2$ as shown in the following equation:

$$3H_3PO_4 + 2SrCO_3 \xrightarrow{\sim 200-250^\circ C} Sr(H_2PO_4)_2 + SrHPO_4 + 2CO_2 + 2H_2O \quad (7)$$

Subsequently, the newly formed $SrHPO_4$ and $Sr(H_2PO_4)_2$ dehydrated at 300–450 °C, as given in Eqs. (3) and (4). The dehydration temperatures were slightly lower than the corresponding values for the case of SrO, indicating that the reactivity of $SrHPO_4$ and $Sr(H_2PO_4)_2$ formed by the reaction of H_3PO_4 with $SrCO_3$ was higher than that formed by the reaction with SrO. The sharp weight loss step at 800–950 °C should be ascribed to both the dehydration accompanied by the solid-state reactions concerning $SrH_2P_2O_7$ as shown in Eq. (6) and decarbonation of remaining $SrCO_3$ to give SrO as shown in Eq. (8), since the DTG profile showed two weight loss peaks. The highly exothermic solid-state reactions between newly generated species took place at 800–1300 °C which resulted in the formation of Sr_2SiO_4 and finally of $Sr_5(PO_4)_2SiO_4$ as shown in Eqs. (5) and (6).

$$SrCO_3 \xrightarrow{\sim 800-950^\circ C} SrO + CO_2 \quad (8)$$

When $Sr(NO_3)_2$ was used as the strontium source, two big endothermic peaks accompanied by sharp weight loss steps appeared at temperature ranges of 180–280 (weight loss 28%), 600–650 °C (weight loss about 15%), respectively. Small weight loss steps were also observed at ~60, 372 and 443 °C. It is interesting to note that the onset of weight loss occurred at 60 °C which was quite lower than that of SrO and $SrCO_3$. This is easily understood. Since both $(NH_4)_2HPO_4$ and $Sr(NO_3)_2$ were active species, the reaction between these two species as given in Eq. (9) could take place during preparing the intimate mixture by thoroughly grounding and milling of the raw materials at room temperature. The mixture might contain some NH_4NO_3 species, which was easily evaporated and decomposed at a low temperature during heating. Hence, the weight loss at 60 °C could be ascribed to the evaporation and/or decomposition of NH_4NO_3 in the mixture.

Based on the TG–DTG–DSC profiles, the main chemical reactions taking place during the heating of the stoichiometric mixture of raw materials using $Sr(NO_3)_2$ as the strontium source were proposed as follows:

The sharp weight loss at ~180–280 °C could be ascribed to the reaction between $(NH_4)_2HPO_4$ and $Sr(NO_3)_2$ shown in Eq. (10), followed by the stepwise decomposition of remaining $Sr(NO_3)_2$ at ~300–450 and 600–650 °C, respectively, in the way given in Eqs. (11) and (12). The SrO generated then reacted with SiO_2 at 800–1300 °C to give Sr_2SiO_4. On the other hand, the $SrHPO_4$ formed at 180–260 °C dehydrated at 300–450 °C to give $Sr_2P_2O_7$ as shown in Eq. (3), which further reacted with SrO and Sr_2SiO_4 leading to the formation of $Sr_5(PO_4)_2SiO_4$ as given in Eq. (13). The fact that no weight loss was observed above 700 °C demonstrated the absence of degradable species of $SrH_2P_2O_7$ in the system. Hence, the solid-state reactions at higher temperature region using $Sr(NO_3)_2$ were different from those using SrO and $SrCO_3$ given in Eq. (6). The DSC curve showed that heat flow at the high temperatures went down more rapidly from the maximum than that of SrO and $SrCO_3$, indicating that the rate of final solid-state reaction leading to the formation of $Sr_5(PO_4)_2SiO_4$ phosphor was relatively faster.

$$(NH_4)_2HPO_4 + Sr(NO_3)_2 \xrightarrow{\text{room-temperature}} SrHPO_4 + 2NH_4NO_3 \quad (9)$$

$$(NH_4)_2HPO_4 + Sr(NO_3)_2 \xrightarrow{\sim 260^\circ C} SrHPO_4 + 2N_2 + O_2 + 4H_2O \quad (10)$$

$$Sr(NO_3)_2 \xrightarrow{\sim 300-400^\circ C} Sr(NO_2)_2 + O_2 \quad (11)$$

$$Sr(NO_2)_2 \xrightarrow{\sim 600-650^\circ C} SrO + NO + NO_2 \quad (12)$$

$$Sr_2SiO_4 + SrO + Sr_2P_2O_7 \xrightarrow{\sim 800-1300^\circ C} Sr_5(PO_4)_2SiO_4 \quad (13)$$

Fig. 2 shows XRD patterns of $Sr_{4.94}(PO_4)_2SiO_4$:$Eu_{0.06}$ phosphors prepared using different sources of strontium. The patterns of the samples were in good agreement with JCPDS files No. 21–1187 of $Sr_5(PO_4)_2SiO_4$ [27]. Meanwhile, small diffraction peaks with two theta degree values at 27.3 and 31.3 corresponding to Sr_2SiO_4 (JCPDS 39–1256) were also observed. The presence of Sr_2SiO_4 for the phosphors prepared from different strontium sources and stoichiometric $(NH_4)_2HPO_4$ may be due to the slow rate of solid-state reaction and volatility of $(NH_4)_2HPO_4$ which make the amount of phosphorus species remaining in the mixture less than stoichiometry at the high temperatures. This also proved the reaction scheme proposed above that Sr_2SiO_4 was the intermediate phase during the formation of the phosphosilicate phosphor. The intensity of Sr_2SiO_4 impurity phase in the phosphor decreased with strontium sources in the order of $SrO > SrCO_3 > Sr(NO_3)_2$. This is easily understood. Since compared with reagent SrO being directly added, the fresh SrO produced in-situ by decomposition of the nitrate or the carbonate during solid-state reaction had smaller particle size and higher reactivity [24]. Moreover, decomposition of $Sr(NO_3)_2$ took place at the temperature significantly lower than that of $SrCO_3$ and the rate of the final solid-state reaction was faster as observed in TG–DTG–DSC profiles. The phase purity of phosphor prepared was high correspondingly.

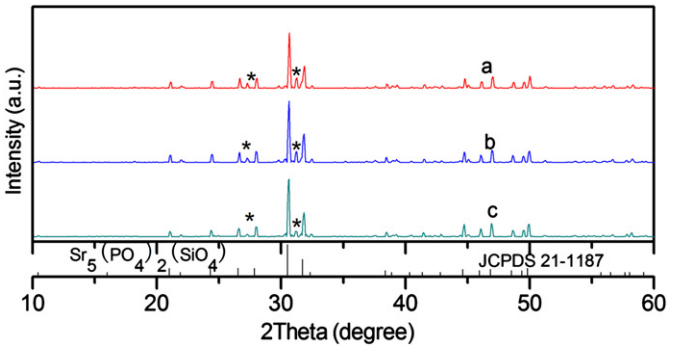

Fig. 2. XRD patterns of $Sr_{4.94}(PO_4)_2SiO_4$:$Eu_{0.06}$ prepared by solid-state reaction with different strontium sources (a) SrO; (b) $SrCO_3$ and (c) $Sr(NO_3)_2$. "*" denotes Sr_2SiO_4 impurity phase.

Fig. 3 shows SEM images of $Sr_{4.94}(PO_4)_2SiO_4$:$Eu_{0.06}$ phosphors prepared by solid-state reaction with different strontium sources. It was found that particle irregularity, particle size and surface roughness of the phosphors prepared from different strontium sources were different. When SrO was used as the strontium source, dense coagulated quasi-spherical particles with a size about 5–10 μm were observed. When $Sr(NO_3)_2$ was used as the strontium source, the particles were egg-like or quasi-spherical with a mean size of ca 2–5 μm. In the case of $SrCO_3$, phosphor particles were in an irregular form with coarse surface and a size of ca 5 μm. The different particle size and morphology of the phosphors were related with not only the particle size of the strontium sources but the specific reaction and nucleation processes. As shown in the thermal analysis, the reaction scheme and weight loss percentage when using the unlike strontium sources were different, indicating that amount (or volume) of volatile species (gas and H_2O) generated and the temperature at which the volatile species was generated in solid-state reactions were different. The release of volatile species in solid-state reaction might form some gas pass-ways (or channels) which prohibited the agglomeration and

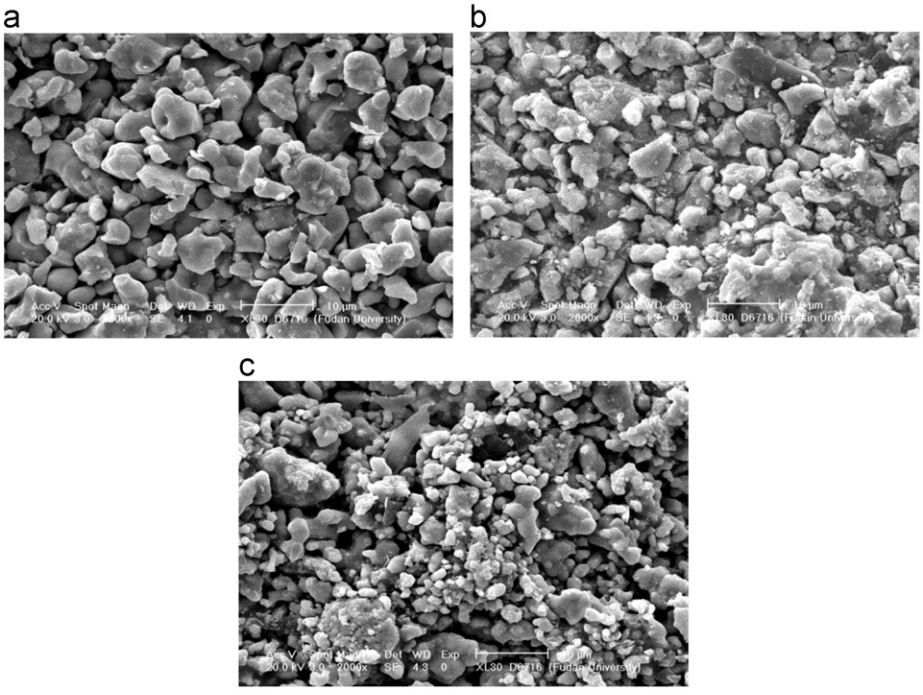

Fig. 3. SEM images of $Sr_{4.94}(PO_4)_2SiO_4$:$Eu_{0.06}$ phosphors prepared with different strontium sources. (a) SrO; (b) $SrCO_3$ and (c)$Sr(NO_3)_2$.

aggregation of the particles, and consequently, led to the formation of dispersed particles with relatively smaller sizes.

Fig. 4 shows PLE and PL spectra of $Sr_{4.94}(PO_4)_2SiO_4:Eu_{0.06}$ phosphors prepared with different strontium source measured at room temperature. The PLE spectra showed a wide absorption band with wavelength ranging from 250 to 420 nm. Under the excitation of 346 nm the phosphors showed a green emission band peaking at wavelength ca 496 nm along with a shoulder at ca 550 nm. The broad excitation and emission band could be assigned to 4f–5d transitions of Eu^{2+} ions [25]. The asymmetric excitation and emission spectra indicated that there was more than one Eu^{2+} emission centers in the lattice. The crystal structure of $Sr_5(PO_4)_2SiO_4$ has been studied and elucidated in the literature [19,20,25,27]. Two sites are available in $Sr_5(PO_4)_2SiO_4$ apatite structure for activator cations, namely the site Sr1 on the 4f position (C_3 point symmetry) with 9-fold coordination and the site Sr2 at the 6 h (Cs symmetry) with 7-fold coordination. The bond length of Sr2–O is shorter than that of Sr1–O. According to site coordination and Eu^{2+} ligand distances of the two sites, the emission at 496 nm should be from Eu^{2+} at 9-fold coordination 4f sites, and the emission around 550 nm should be from the Eu^{2+} at 7-fold coordination 6 h sites which experienced stronger crystal field owing to shorter distance between Eu^{2+} and the nearest anions. The peak wavelength of the emission being slightly different from the literature value should be due to different Eu^{2+} doping concentrations, since the emission of Eu^{2+} in apatite is concentration dependent [20]. XRD results in Fig. 2 showed that trace of Sr_2SiO_4 impurity phase was also present in the phosphor. However, it is hard to separate the emission from Eu^{2+} in the silicate. Because the content of Sr_2SiO_4 phase was very low and the emission of Eu^{2+} in Sr_2SiO_4 was around 550 nm [8] which is overlapped with the emission of Eu^{2+} at 7-fold coordination 6h sites. Comparison of the PL spectra of the phosphors prepared from different strontium sources revealed that the emission intensity was positively correlated with the phase purity of the phosphosilicate apatite phosphor.

3.2. Effect of phosphorus sources

$(NH_4)_2HPO_4$ was commonly used as a phosphorus source when preparing phosphate and phosphosilicate phosphors [12,16,28]. In preparation of halophosphate phosphors alkaline earth monophosphate $MHPO_4$ was often used [29,30]. In this paper, $SrHPO_4$ and $(NH_4)_2HPO_4$ were employed as the phosphorus sources for comparison and using $SrCO_3$ as the strontium source. The reason for using $SrCO_3$ instead of more reactive $Sr(NO_3)_2$ as the strontium source here was for environmental consideration since nitric oxides would be generated during the heating of the mixture containing $Sr(NO_3)_2$. To compensate for the evaporation of $(NH_4)_2HPO_4$ species in high-temperature solid-state reactions, excess $(NH_4)_2HPO_4$ was added. We expected to explore whether it is possible to improve the phase purity of apatite by adding excess $(NH_4)_2HPO_4$. The reactivity and reaction scheme of the intimate mixture with a formula of $Sr_{4.94}(PO_4)_2SiO_4:Eu_{0.06}$ using stoichiometric $SrHPO_4$ or $(NH_4)_2HPO_4$ as the phosphorus source was studied by TA. In Fig. 5 TG–DTG–DSC profiles of the mixture using $SrHPO_4$ as the phosphorus source are shown. The TG–DTG–DSC profiles of the stoichiometric mixture using $(NH_4)_2HPO_4$ as the phosphorus source were same as the case discussed in the previous section about $SrCO_3$.

It was seen from Fig. 5 that weight loss steps occurred at 310–350 (about 3%) and 800–1000 °C (about 10%). The weight loss at 800–1000 °C proceeded in two-step. Based on the thermodynamics of $SrHPO_4$ and $SrCO_3$ and the

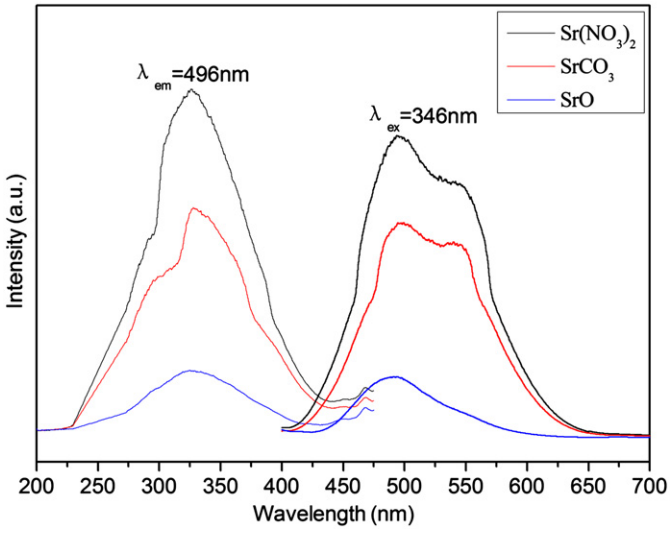

Fig. 4. PLE and PL spectra of $Sr_{4.94}(PO_4)_2SiO_4:Eu_{0.06}$ phosphors prepared with different strontium sources.

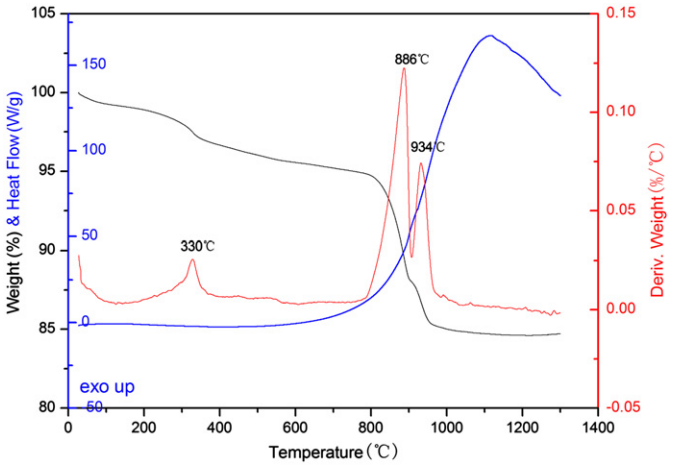

Fig. 5. TG–DTG–DSC profiles of stoichiometric mixture of raw materials using $SrHPO_4$ as the phosphorus source.

TG–DTG–DSC curves, the main reactions taking place during the heating of the mixture using $SrHPO_4$ as the phosphorus source were proposed as follows:

The weight loss step at temperature range 310–350 °C should be ascribed to the dehydration of $SrHPO_4$ to form $Sr_2P_2O_7$ as shown in Eq. (3). The temperature of $SrHPO_4$ dehydration was similar to the corresponding values of $SrCO_3$ in Fig. 1, indicating that $SrHPO_4$ directly added might be in the same modification with that generated in-situ by solid-state reactions of H_3PO_4 with $SrCO_3$. According to the literature, $SrHPO_4$ has alpha and beta modifications [26]. The two weight loss steps at 800–1000 °C should be due to the decarbonation of $SrCO_3$ as given in Eq. (8) and the reaction of $Sr_2P_2O_7$ with $SrCO_3$ as given in Eq. (14). The generated SrO by decarbonation of $SrCO_3$ then reacted with SiO_2 to form Sr_2SiO_4 which further reacted with $Sr_3(PO_4)_2$ resulting in the formation of $Sr_5(PO_4)_2SiO_4$ phosphor as shown in Eq. (15). The DSC profile indicated that in contrast with the flat peak between 1000 and 1300 °C when using $(NH_4)_2HPO_4$ phosphorus source in Fig. 1, a tower-shape DSC profile appeared for the mixture using $SrHPO_4$, indicating that the rate of the final exothermic solid-state reactions was faster than that of any samples in Fig. 1.

$$Sr_2P_2O_7 + SrCO_3 \overset{\sim 800-900\ ^\circ C}{\longrightarrow} Sr_3(PO_4)_2 + CO_2 \quad (14)$$

$$Sr_2SiO_4 + Sr_3(PO)_2 \overset{\sim 900-1300\ ^\circ C}{\longrightarrow} Sr_5(PO_4)_2SiO_4 \quad (15)$$

Fig. 6 shows XRD patterns of the $Sr_{4.94}(PO_4)_2SiO_4:Eu_{0.06}$ phosphors prepared from different source of phosphorus. The patterns showed that phosphors were composed of $Sr_5(PO_4)_2SiO_4$ apatite phase (JCPDS 21–1187) and trace amount of impurity Sr_2SiO_4. When $(NH_4)_2HPO_4$ was used as the phosphorus source, the intensity of the Sr_2SiO_4 impurity phase decreased obviously with the addition of excess $(NH_4)_2HPO_4$ in the mixture. When 5% excess of $(NH_4)_2HPO_4$ was added, the silicate impurity phase was not detected. On the other hand, the Sr_2SiO_4 impurity phase was hardly detected when $SrHPO_4$ was used in a stoichiometric ratio. This may be related with not only the lower volatility of $SrHPO_4$ than $(NH_4)_2HPO_4$ but also the different reaction schemes as discussed in the thermal analysis section.

Fig. 7 shows SEM images of the $Sr_{4.94}(PO_4)_2SiO_4:Eu_{0.06}$ phosphors prepared by solid-state reaction from different source of phosphorus. It was found that the morphology and particle size of the phosphor prepared with a stoichiometric $SrHPO_4$ were similar to that using a stoichiometric $(NH_4)_2HPO_4$, both in a coarse irregular form with a size of ca 5–10 μm. When $(NH_4)_2HPO_4$ was used with 3% excess, the surface smoothness of the phosphor were improved obviously, but the average particle size was decreased. When $(NH_4)_2HPO_4$ was used with 5% excess, aggregation of phosphor particles occurred, and mean particle size was increased slightly.

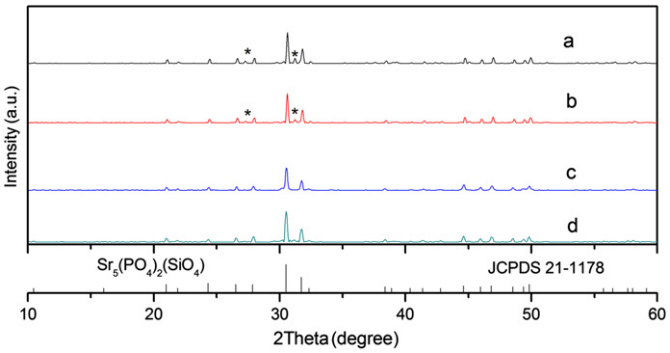

Fig. 6. XRD patterns of $Sr_{4.94}(PO_4)_2SiO_4:Eu_{0.06}$ phosphors prepared using $(NH_4)_2HPO_4$ and $SrHPO_4$ as the phosphorus source. (a) $(NH_4)_2HPO_4$ in stoichiometric ratio; (b) $(NH_4)_2HPO_4$ with 3% excess; (c) $(NH_4)_2HPO_4$ with 5% excess and (d) $SrHPO_4$ in stoichiometric ratio. "*" denotes Sr_2SiO_4 impurity phase.

Fig. 8 shows PLE and PL spectra of the $Sr_{4.94}(PO_4)_2SiO_4:Eu_{0.06}$ phosphors prepared by solid-state reaction with $SrHPO_4$ and $(NH_4)_2HPO_4$ as the source of phosphorus, respectively. It was found that the source of phosphorus had little influence on the spectral shape of PLE and PL, but the intensities of the excitation and emission changed significantly. When $(NH_4)_2HPO_4$ was used as the phosphorus source, the emission intensity at ca 496 nm increased obviously with addition of 3% excess $(NH_4)_2HPO_4$, further increasing $(NH_4)_2HPO_4$ content to 5% excess resulted in only slight improvement in emission intensity at 496 nm. The intensity of emission around 550 nm increased steadily with the content of $(NH_4)_2HPO_4$ in the mixture in the cases studied. When $SrHPO_4$ was used as the phosphorus source in a stoichiometric ratio, the PL emission intensity of the phosphor was higher than that prepared from $(NH_4)_2HPO_4$ phosphorus source. The enhanced emission intensity of the phosphors with a stoichiometric $SrHPO_4$ or with excess of $(NH_4)_2HPO_4$ may be attributed mainly to the improved phase purity of the phosphors as observed in Fig. 6. On the other hand, the particle size and morphology of the phosphors may influence the reflection and absorption ratio of incident excitation radiation, which consequently affected the PL and PLE intensity of the phosphor. This should be the reason that the phosphor prepared with $SrHPO_4$ showed higher emission intensity than that prepared with excessive $(NH_4)_2HPO_4$ that had the same phase purity.

4. Summary

$Sr_{4.94}(PO_4)_2SiO_4:Eu_{0.06}$ phosphor was prepared by high temperature solid-state reaction. Effects of strontium and phosphorus sources on the reactivity of their mixture and on phase composition, morphology and PL and PLE of the phosphors were investigated. For the strontium source, SrO generated in-situ by decomposition of nitrate or carbonate during solid-state reactions showed higher reactivity than that

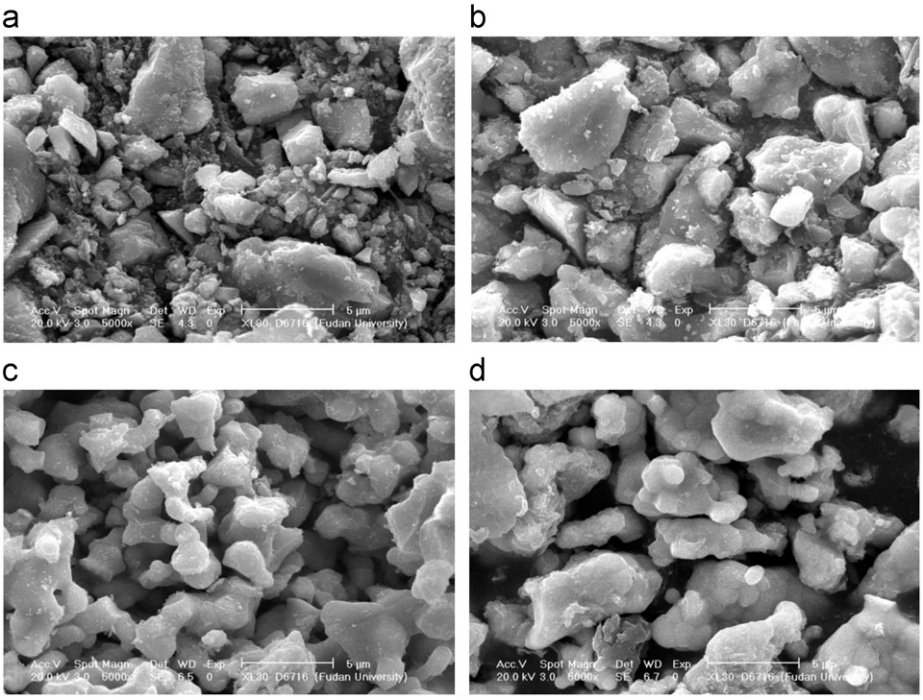

Fig. 7. SEM images of $Sr_{4.94}(PO_4)_2SiO_4:Eu_{0.06}$ phosphors prepared with different phosphorus sources. (a) $SrHPO_4$ in stoichiometric ratio; (b) $(NH_4)_2HPO_4$ in stoichiometric ratio; (c) $(NH_4)_2HPO_4$ with 3% excess and (d) $(NH_4)_2HPO_4$ with 5% excess.

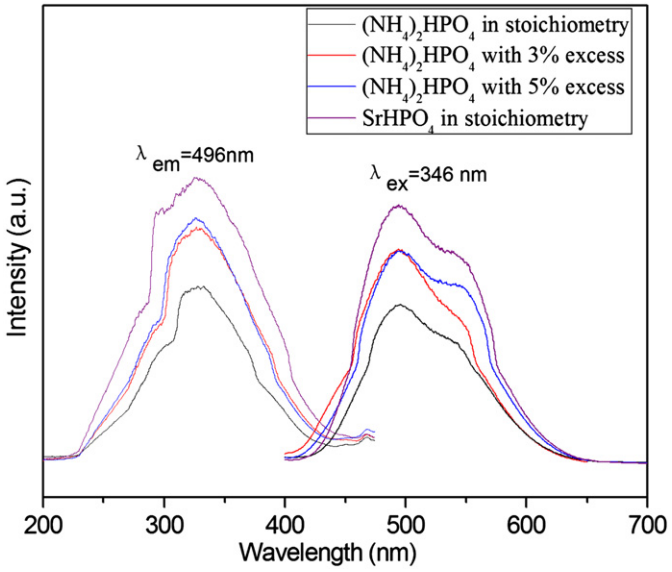

Fig. 8. PLE and PL spectra of $Sr_{4.94}(PO_4)_2SiO_4:Eu_{0.06}$ phosphors prepared using stoichiometric $SrHPO_4$ and different amounts of $(NH_4)_2HPO_4$ as the phosphorus source, respectively.

of reagent SrO directly added, the phase purity of the apatite phosphors prepared from the strontium salts was better than that using SrO. The phosphors prepared from the strontium salts also exhibited smaller particle size and less aggregation and hence higher PLE and PL intensity than that using SrO. Due to both the volatility of $(NH_4)_2HPO_4$ and low reactivity of SiO_2 it was hard to prepare pure phase phosphosilicate phosphor with a stoichiometric $(NH_4)_2HPO_4$ as the phosphorus source. Minor Sr_2SiO_4 impurity phase was detected in the phosphors. The phase purity of the phosphor was improved with the addition of excess $(NH_4)_2HPO_4$. When $(NH_4)_2HPO_4$ with 5% excess was used as the phosphorus source, the impurity phase was not detected. On the other hand, when stoichiometric $SrHPO_4$ was used as the phosphorus source, the pure phase phosphosilicate phosphor was obtained. The phosphor showed higher PL and PLE intensity than that prepared from $(NH_4)_2HPO_4$ phosphorus source.

References

[1] S. Nakamura, S. Pearton, G. Fasol, The Blue Laser Diode, second updated and extended ed., Springer, Berlin, 1996, p. 230.
[2] R.-J. Xie, Y.Q. Li, N. Hirosaki, H. Yamamoto, Nitride Phosphors and Solid-State Lighting, CRC Press, New York, 2011.
[3] A.A. Setlur, H.A. Comanzo, A.M. Srivastava, Spectroscopic evaluation of a white light phosphor for UV–LEDs-$Ca_2NaMg_2V_3O_{12}:Eu^{3+}$, Journal of the Electrochemical Society 152 (2005) H205–H208.
[4] W.J. Yang, L. Luo, T.M. Chen, N.S. Wang, Luminescence and energy transfer of Eu–Mn-coactivated $CaAl_2Si_2O_8$ as a potential phosphor for white-light UV–LED, Chemistry of Materials 17 (2005) 3883–3888.
[5] S. Ye, Z.S. Liu, X.T. Wang, J.G. Wang, L.X. Wang, X.P. Jing, Emission properties of Eu^{2+}, Mn^{2+} in $MAl_2Si_2O_8$ (M=Sr, Ba), Journal of Luminescence 129 (2009) 50–54.
[6] J.S. Kim, P.Y. Jeon, J.C. Choi, H.L. Park, S.I. Mho, G.C. Kim, Warm-white-light emitting diode utilizing a single-phase full-color $Ba_3MgSi_2O_8:Eu^{2+}$, Mn^{2+} phosphor, Applied Physics Letters 84 (2004) 2931–2933.
[7] Y. Umetsu, S. Okamoto, H. Yamamoto, Photoluminescence properties of $Ba_3MgSi_2O_8:Eu^{2+}$ phosphor and $Ba_3MgSi_2O_8:Eu^{2+}$, Mn^{2+}

blue–red phosphor under near-ultraviolet-light excitation, Journal of the Electrochemical Society 155 (2008) J193–J197.
[8] S.H. Lee, H.Y. Koo, Y.C. Kang, Characteristics of α′- and β-Sr_2SiO_4:Eu^{2+} phosphor powders prepared by spray pyrolysis, Ceramics International 36 (2010) 1233–1238.
[9] L. Chen, C.C. Lin, C.W. Yeh, R.S. Liu, Rare-earth activated nitride phosphors: synthesis, luminescence and applications, Materials 3 (2010) 2172–2195.
[10] C.C. Lin, R.-S. Liu, Advances in phosphors for light-emitting diodes, Journal of Physical Chemistry Letters 2 (2011) 1268–1277.
[11] H.A. Hoppe, M. Daub, M.C. Brohmer, Coactivation of α-$Sr(PO_3)_2$ and $SrM(P_2O_7)$ (M=Zn, Sr) with Eu^{2+} and Mn^2, Chemistry of Materials 19 (2007) 6358–6362.
[12] Z. Wua, J. Liu, M. Gong, Thermally stable luminescence of $SrMg_2(PO_4)_2$: Eu^{2+} phosphor for white light NUV light-emitting diodes, Chemical Physics Letters 466 (2008) 88–90.
[13] N. Guo, Y. Zheng, Y. Jia, H. Qiao, H. You, Warm-white-emitting from Eu^{2+}/Mn^{2+}-codoped $Sr_3Lu(PO_4)_3$, Journal of Physical Chemistry C 116 (2012) 1329–1334.
[14] C. Zhao, X. Yin, Y. Wang, F. Huang, Y. Hang, Photoluminescence properties of $Ca_9Lu(PO_4)_7$:Ce^{3+}, Mn^{2+} prepared by conventional solid-state reaction, Journal of Luminescence 132 (2012) 617–621.
[15] C.C. Lin, Z.R. Xiao, G.Y. Guo, T.S. Chan, R.S. Liu, Versatile phosphate phosphors $ABPO_4$ in white light-emitting diodes: collocated characteristic analysis and theoretical calculations, Journal of the American Chemical Society 132 (2010) 3020–3028.
[16] C.F. Guo, L. Luan, X. Ding, D.X. Huang, Luminescent properties of $SrMg_2(PO_4)_2$: Eu^{2+}, and Mn^{2+} as a potential phosphor for ultraviolet light-emitting diodes, Applied Physics A 91 (2008) 327–331.
[17] S.R. Yan, X.F. Hu, H.H. Fei, J.G. Hu, G.J. Wan, L. Ma, Preparation and properties of Eu^{2+}-activated alkaline-earth phosphosilicate phosphors, Solid State Communications 148 (2008) 186–189.
[18] H.S. Roh, S. Hur, H.J. Song, I.J. Park, D.K. Yim, D.W. Kim, K.S. Hong, Luminescence properties of $Ca_5(PO_4)_2SiO_4$:Eu^{2+} green phosphor for near UV-based white LED, Materials Letters 70 (2012) 37–39.
[19] J.H. Gan, Y.L. Huang, L. Shi, X.B. Qiao, H.J. Seo, Luminescence properties of Eu^{2+}-activated $Sr_5(PO_4)_2(SiO_4)$ for green-emitting phosphor, Materials Letters 63 (2009) 2160–2162.
[20] X.G. Wang, J.H. Gan, Y.L. Huang, H.J. Seo, The doping concentration dependent tunable yellow luminescence of $Sr_5(PO_4)_2$ (SiO_4):Eu, Ceramics International 38 (2012) 701–706.
[21] Y. Huang, J. Gan, R. Zhu, X. Wang, H.J. Seo, Structural phase formation and tunable luminescence of Eu^{2+}-activated apatite-type $(Ca,Sr,Ba)_5(PO_4)_2(SiO_4)$, Journal of the Electrochemical Society 158 (2011) J334–J340.
[22] J. Yu, W. Gong, Z. Xiao, G. Ning, Spectral structure of barium, phosphate, silicate phosphor $Ba_{10}(PO_4)_4(SiO_4)_2$:Eu, M^+, Journal of Luminescence 132 (2012) 2957–2960.
[23] P.F. Smet, A.B. Parmentier, D. Poelman, Selecting conversion phosphors for white light-emitting diodes, Journal of the Electrochemical Society 158 (2011) R37–R54.
[24] R.C. Ropp, Luminescence and the solid state, second ed., Elsevier, Amsterdam, 2004, p. 121.
[25] G. Blasse, A. Bril, Energy transfer between Eu^{2+} ions in non-equivalent sites in strontium–silicate–phosphate, Physics Letters A 28 (1969) 572–573.
[26] R.W. Mooney, M.A. Aia, Chemical Reviews 61 (1961) 433–462.
[27] V.H. Schwarz, Strontiumapatite des Typs $Sr_{10}(PO_4)_4(X^{IV}O_4)_2$ (X^{IV}=Si, Ge), Zeitschrift für anorganische und allgemeine Chemie 357 (1968) 43–53.
[28] J. Wang, S. Wang, Q. Su, Synthesis, photoluminescence and thermo stimulated -luminescence properties of novel red long-lasting phosphorescent materials β-$Zn_3(PO_4)_2$:Mn^{2+}, M^{3+}(M=Al and Ga), Journal of Materials Chemistry 14 (2004) 2569–2574.
[29] M. Kottaisamy, M. Mohan Rao, D. Jeyakumar, Divalent europium-activated alkaline-earth-metal chlorophosphate luminophores [$M_5(PO_4)_3Cl$:Eu^{2+}; M=Ca, Sr, Ba] by self-propagating high-temperature synthesis, Journal of Materials Chemistry 7 (1997) 345–349.
[30] M.H. Hwang, E.Y. Lee, S.-H. Hong, Y.-B. Sun, Y.J. Kim, Preparation and luminescent properties of $Ca_5(PO_4)_3Cl$:Eu^{2+} phosphors by a solid-state reaction method, Journal of the Electrochemical Society 156 (2009) J185–J188.